Int. J. Therm. Sci. (1999) 38, 560–571
© Elsevier, Paris

Positivity preservation and adaptive solution of two-equation models of turbulence

Florin Ilinca[a], Dominique Pelletier[b*]

[a] *Industrial Materials Institute, National Research Council, 75, de Mortagne, Boucherville, Québec, Canada, J4B 6Y4*
[b] *École Polytechnique de Montréal, Case postale 6079, succ. centre-ville, Montréal, Québec, Canada, H3C 3A7*

(Received 2 March 1998, accepted 22 December 1998)

Abstract — This paper proposes a simple change of dependent variables that guarantees positivity of turbulence variables in numerical simulation codes. The approach consists in solving for the natural logarithm of the turbulence variables which are known to be strictly positive. The approach is valid for any numerical scheme be it a finite difference, a finite volume, or a finite element method. The paper presents the turbulence equations in logarithmic variables for two popular turbulence models: the standard k–ε model and the k–ω model of Wilcox. The advantages of the proposed formulation and the associated numerical difficulties are discussed within the framework of an adaptive finite element method. Error estimation and mesh adaptation procedures are described. The approach is applied to flows for which analytical solution or experimental measurements are available: a shear layer and the flow over a backward facing step. The proposed approach results in a robust adaptive algorithm. Predictions compare well with measurements. © Elsevier, Paris.

positivity preservation / turbulent flows / Navier-Stokes / two-equation models / error estimation / adaptivity / logarithmic variables

Résumé — **Préservation de la positivité et solution adaptative des modèles de turbulence à deux équations.** Nous proposons dans cet article un changement de variable garantissant la positivité des variables de turbulence dans les codes de simulation numérique. L'approche utilise le logarithme naturel des variables de turbulence comme variable de calcul. Cette approche est valide, quel que soit le schéma numérique utilisé, qu'il s'agisse de différences, de volumes ou d'éléments finis. L'article présente les équations différentielles en variables logarithmiques pour deux modèles de turbulence courants : le modèle k–ε standard et le modèle k–ω de Wilcox. Nous discutons des avantages de la nouvelle formulation, ainsi que des difficultés qui y sont associées, le tout dans un cadre d'adaptation de maillage. Nous décrivons l'estimation d'erreur et la méthode d'éléments finis adaptative. Nous appliquons la méthode à deux cas pour lesquels, soit il existe une solution analytique, soit des mesures expérimentales sont disponibles. Il s'agit d'une couche cisaillée et de l'écoulement sur une marche descendante. L'approche proposée s'avère robuste. Les prédictions se comparent avantageusement aux résultats expérimentaux. © Elsevier, Paris.

positivité / écoulements turbulents /modèles à deux équations / adaptativité / éléments finis

Nomenclature

e	error	
E	roughness parameter	
κ	Von Karman constant	
$\boldsymbol{f}$	body force	$\mathrm{N\cdot kg^{-1}}$
h	element size	
p	pressure	Pa
Pe	Péclet number	
$P(\boldsymbol{u})$	production term	$\mathrm{s^{-2}}$
q	solution derivative	
$\boldsymbol{u}$	velocity vector	$\mathrm{m\cdot s^{-1}}$
k	turbulence kinetic energy (TKE)	$\mathrm{m^2\cdot s^{-2}}$
$\mathcal{K}$	natural logarithm of the TKE	
ε	turbulence dissipation rate	$\mathrm{m^2\cdot s^{-3}}$
$\mathcal{E}$	natural logarithm of ε	
ω	specific turbulence dissipation rate	$\mathrm{s^{-1}}$
Ω	natural logarithm of ω	
μ	viscosity	$\mathrm{kg\cdot m^{-1}s^{-1}}$
ρ	density	$\mathrm{kg\cdot m^{-3}}$
σ_k	turbulence kinetic Prandl number	
σ_ε	turbulence dissipation Prandtl number	
τ	stabilization parameter	

* Correspondence and reprints.

τ_w	wall shear stress.....	$N \cdot m^{-2}$
∇	gradient operator	
$\nabla \cdot$	divergence	

Subscripts

h	finite element solution
ex	exact solution
T	turbulent
w	values on the boundary

1. INTRODUCTION

Adaptive methods are a powerful tool for solving complex computational fluid dynamics problems. This is especially true for two-equation models of turbulence. The coupled system of differential equations is very stiff and the solutions present sharp internal layers and fronts whose location is difficult to assess a priori. Yet, achieving adequate numerical resolution of such features is critical to the accuracy of the numerical predictions. Another major hurdle is ensuring that turbulence variables remain positive (k, ε, ω) throughout the domain and during the course of iterations. Failure to ensure this condition can result in immediate and irrecoverable breakdown of iterations.

Various approaches have been devised to deal with this problem, ranging from the implementation of clipping operators or limiters [1–3], the design of special upwind finite volume schemes [4, 5], the use of discretization schemes that promote positivity [5, 6] or even guarantee it [7], to the design of turbulence models less prone to this kind of breakdown [8, 9]. The last approach presents the drawback of possibly imposing limitations on the turbulence modeling effort with the result that some potentially useful mathematical model might be discarded because the numerical scheme cannot handle it properly. Upwind schemes have shown good potential in finite volume algorithms. However, upwind schemes cannot guarantee positivity under all circumstances. Positivity promoting algorithms are usually designed on a case by case basis since their structure depends in part on the turbulence model that has been retained. Use of solution clipping and limiters is very wide spread but it does have two drawbacks. First, it slows down the convergence of the iterative solver because clipped values of the solution destroy the residuals of the solution. Secondly, clipping introduces noises and oscillations in the solution fields. Negative values that are locally reset to some small positive values can result in locally very large solution gradients and curvature, even if the values of k and ε or ω are small. An adaptive algorithm will tend to cluster grid points in these regions with the net result that the mesh is being adapted to the inability of the solver to produce a smooth and positive solution rather than refining the grid in regions of large solution curvature.

Thus, there is a need to improve the quality of the flow solver in order to fully benefit from the potential offered by adaptive methods. This paper presents a change of dependent variables for turbulence quantities that results in improved solution quality (smoothness) so that quantitative improvements by adaptive remeshing can be fully realized. The computational variables are the natural logarithm of k, ε, and ω. This choice offers several advantages. First, the eddy viscosity and the turbulence variables are always positive since they are obtained by taking the exponential of the appropriate computational variables. Second, it leads to improved accuracy in regions of rapid variations of the solution because the logarithm varies more slowly than its argument. This last property also makes it possible to obtain solutions on coarser meshes because the logarithmic variables act as modified interpolation functions better suited to such situations. Finally, solution accuracy is also improved in regions of very low turbulence levels. The cost incurred for these benefits is a mild increase of the nonlinearity of the system of partial differential equations to be solved.

The paper is organized as follows. Section 1 presents the Reynolds-averaged Navier-Stokes equations and the turbulence equations for the standard k–ε model [10] and the k–ω model of Wilcox [11]. Section 2 discusses the change of variables leading to the logarithmic variable form of the turbulence equations, and also some of the advantages for using such variables. Section 3 presents the finite element formulation for solving the transformed equations. Section 4 presents the error estimation and adaptive strategies used in conjunction with the new equations and finite element methods. Here again advantages of the new formulation in regards to adaptivity are discussed: solution smoothness, eddy viscosity representation, robustness in region of low turbulence. Section 5 compares the various approaches and methods on problems for which a closed form solution or experimental data are available. The paper ends with conclusions.

2. MODELING OF THE PROBLEM

2.1. Reynolds-averaged Navier-Stokes equations

The flow regime of interest is modeled by the Reynolds-averaged Navier-Stokes equations:

$$\rho \mathbf{u} \cdot \nabla \mathbf{u} = -\nabla p + \nabla \cdot [(\mu + \mu_T)(\nabla \mathbf{u} + \nabla \mathbf{u}^T)] + \rho \mathbf{f}$$

$$\nabla \cdot \mathbf{u} = 0$$

where ρ is the density, μ is the fluid viscosity and $\mathbf{f}$ is a body force. The turbulent viscosity μ_T is computed using the k–ε model of turbulence:

$$\mu_T = \rho C_\mu \frac{k^2}{\varepsilon}$$

or using the k–ω model of turbulence:

$$\mu_T = \rho \frac{k}{\omega}$$

The system is closed by including the transport equations for the turbulence quantities.

2.2. The standard k–ε model

For this model the turbulence quantities are the turbulence kinetic energy, k, and its dissipation rate, ε, which are governed by the following transport equations:

$$\rho\, \mathbf{u}\cdot\nabla k = \nabla\cdot\left[\left(\mu + \frac{\mu_T}{\sigma_k}\right)\nabla k\right] + \mu_T\, P(\mathbf{u}) - \rho\,\varepsilon$$

$$\rho\, \mathbf{u}\cdot\nabla \varepsilon = \nabla\cdot\left[\left(\mu + \frac{\mu_T}{\sigma_\varepsilon}\right)\nabla \varepsilon\right] + C_{\varepsilon 1}\frac{\varepsilon}{k}\mu_T\, P(\mathbf{u}) - C_{\varepsilon 2}\,\rho\,\frac{\varepsilon^2}{k}$$

where the production of turbulence is defined as:

$$P(\mathbf{u}) = \nabla\mathbf{u} : (\nabla\mathbf{u} + \nabla\mathbf{u}^T)$$

The constants σ_k, σ_ε, $C_{\varepsilon 1}$, $C_{\varepsilon 2}$, C_μ take on the standard values proposed by Launder and Spalding [10].

To increase the robustness of the finite element scheme, the equations for k and ε are rewritten by using the eddy viscosity definition [2, 12]. Thus, ε may be rewritten as:

$$\varepsilon = \rho\, C_\mu \frac{k^2}{\mu_T}$$

to achieve the following block-triangular form of the turbulence equations:

$$\rho\, \mathbf{u}\cdot\nabla k = \nabla\cdot\left[\left(\mu + \frac{\mu_T}{\sigma_k}\right)\nabla k\right] + \mu_T\, P(\mathbf{u}) - \rho^2\, C_\mu \frac{k^2}{\mu_T}$$

$$\rho\, \mathbf{u}\cdot\nabla \varepsilon = \nabla\cdot\left[\left(\mu + \frac{\mu_T}{\sigma_\varepsilon}\right)\nabla \varepsilon\right] + \rho\, C_{\varepsilon 1}\, C_\mu\, k\, P(\mathbf{u}) - C_{\varepsilon 2}\,\rho\,\frac{\varepsilon^2}{k}$$

The above equations can now be solved in the following partly segregated manner:

1) given initial conditions $\mathbf{u}_0$, k_0 and ε_0
2) compute μ_T from k and ε
3) for μ_T given
   3.1) solve momentum and continuity
   3.2) solve the k-equation
   3.3) solve the ε-equation
   3.4) update μ_T and goto 3.

In this algorithm step 3.1 consists in solving the Navier-Stokes equations with variable viscosity, a problem for which the proposed adaptive strategy has already proven successful [13, 14]. Steps 3.1 to 3.3 are solved in a Gauss-Seidel fashion, each step using the most recently available values for all variables. Note that, in this form of the algorithm, the only nonlinearities are quadratic ones due to the terms $\mathbf{u}\cdot\nabla\mathbf{u}$, k^2 and ε^2 which are easily treated with Newton's method. Finally, sub-iterations of steps 3.2–3.4 are used to accelerate the overall convergence of the iterative process.

2.3. The k–ω model of Wilcox

For this model the dependent variables are the turbulence kinetic energy, k, and its specific dissipation rate ω [11]:

$$\rho\, \mathbf{u}\cdot\nabla k = \nabla\cdot\left[(\mu + \sigma^*\mu_T)\,\nabla k\right] + \mu_T\, P(\mathbf{u}) - \beta^*\,\rho\, k\,\omega$$

$$\rho\, \mathbf{u}\cdot\nabla \omega = \nabla\cdot\left[(\mu + \sigma\,\mu_T)\,\nabla \omega\right] + \alpha\frac{\omega}{k}\mu_T\, P(\mathbf{u}) - \beta\,\rho\,\omega^2$$

The constants take on the values proposed by Wilcox [11]:

$$\sigma^* = \frac{1}{2}\,,\quad \sigma = \frac{1}{2}\,,\quad \alpha = \frac{5}{9}\,,\quad \beta = \frac{3}{40}\,,\quad \beta^* = \frac{9}{100}$$

The k–ω model equations are solved in the same partly segregated manner described in the previous section. The observations made previously for the k–ε model also apply to the k–ω model.

2.4. Wall Boundary Conditions

On the boundary, a combination of Neumann and Dirichlet conditions are imposed using wall functions which describe the asymptotic behavior of the different variables near a solid wall [10]. For the turbulence kinetic energy we set the normal derivative at the wall to zero [15], so the TKE values on boundary points k_w are computed as part of the solution. Then we impose the wall shear stress through:

$$\tau_w = \frac{\rho\, U\, C_\mu^{1/4}\, k_w^{1/2}}{U^+}$$

where

$$U^+ = \begin{cases} y^+ & ,\quad y^+ < y_c^+ \\ \dfrac{1}{\kappa}\ln(E y^+) & ,\quad y^+ \geq y_c^+ \end{cases}$$

$$y^+ = \frac{\rho\, C_\mu^{1/4}\, k_w^{1/2}\, y}{\mu}$$

Here, U is the norm of the velocity, y is the distance between the computational boundary and the wall, κ is the Von Karman constant, and E is a roughness parameter ($E = 9.0$ for smooth walls). Finally, the dissipation rate of the TKE, ε, and the specific dissipation rate, ω, on the boundary points are given by

$$\varepsilon_w = \frac{C_\mu^{3/4}\, k_w^{3/2}}{\kappa\, y}\,,\qquad \omega_w = \frac{k_w^{1/2}}{C_\mu^{1/4}\,\kappa\, y}$$

2.5. Limiters for turbulence variables

We now briefly discuss a limiting procedure that we have used with some limited success for solving the k–ε turbulence equations. The turbulence equations contain divisions by k, ε and μ_T. Hence, negative or small values of the denominator can lead to improper sign or overly large values for μ_T or for some source terms. A negative value for the eddy viscosity always has catastrophic effects on the solution and the solver because it makes the equations hyperbolic. Here, both k and ε are limited from below to prevent them from taking overly small values [1, 2]. If k is too small, it is replaced by $k = \frac{k_{\max}}{d_k}$ where $k_{\max}$ is the maximum value found in the domain and d_k is a user supplied constant. If ε is too small and results in overly large values of μ_T, it is replaced by $\varepsilon = \rho C_\mu \frac{k^2}{d_\mu \mu_l}$ where d_μ is a user supplied constant establishing the lower bound of μ_T as $d_\mu \mu_l$. Here μ_l is the fluid viscosity. When quadratic interpolation functions are used we might have positive nodal values for k and ε for which the solution become negative inside the element. Hence, turbulence variables must also be limited from below at integration points [1, 2].

3. POSITIVITY PRESERVING APPROACHES

While the above described technique provides a useful tool for solving turbulent flows, it presents a number of drawbacks. First, the iteration process is quite sensitive to the mesh. Most often, fairly fine meshes must be used to ensure that enough resolution is provided to obtain smooth solutions [1, 2]. This can be quite expensive especially in three dimensions. Second, the clipping process used to enforce positivity results in local oscillations in the turbulence fields. This is very detrimental to the adaptive process since the error estimation technique, described later in the paper, detects these ripples and mistakenly identifies them as regions requiring mesh refinement. The net result is that adaptation is most often wasted on wiggles generated by the solver rather than being applied to improve accuracy in regions of large solution curvature. Regions that do require mesh refinement may be overlooked with the consequence that it is sometimes impossible to obtain a solution on the adapted mesh because the flow solver diverges. In other words, the mesh adaptation is being driven by deficiencies in the flow solver rather than by the flow physics.

The usual fix consists in designing an initial mesh that is sufficiently fine that ripples will be nearly absent, thus defeating the original purpose of the mesh adaptation process. Such symptoms are most clearly seen in free shear flows when both turbulence variable decrease asymptotically towards zero but at such rates that the eddy viscosity asymptotes to some small but constant value which often is several orders of magnitude larger than the turbulence variables themselves [2]. This phenomenon has also been observed, for the case of internal flow over a backward facing step, in the shear layer emanating from the step corner [1]. In this layer all turbulence variables, including the eddy viscosity, present very sharp fronts across which the variables decrease by several orders of magnitude to approach very small values. Wiggles on the side of small values can lead to negative values of k, ε, or the eddy viscosity inside an element. Clipping is triggered in these region with the effect of introducing additional kinks in the solution. Clipping can also result in mesh refinement next to fronts rather than across them.

A simple approach to preserve positivity of the dependent variables consists in solving for their logarithms [16]. This can be viewed as using the following change of dependent variables:

$$\mathcal{K} = \ln k\,, \qquad \mathcal{E} = \ln \varepsilon\,, \qquad \Omega = \ln \omega$$

Solving for the logarithms, (say for example $\mathcal{K}$ and $\mathcal{E}$), guarantees that the turbulence quantities of interest (namely k and ε) will remain positive throughout the computations. Hence the eddy viscosity μ_T will always remain positive. We refer to this approach as solving for **logarithmic variables**. The use of the logarithm of a dependent variable has already been done in order to ensure positivity. Bristeau et al. [17] and Fortin et al. [18] used the logarithm of the density as a dependent variable, instead of the density itself, for solving compressible flows. This guarantees that the density will always be positive. Applied to the transport equations of turbulence variables the technique presents another advantage. Any given field of a turbulence quantity presents very large variation of amplitude across very steep fronts which are difficult to resolve accurately. The fields of the logarithmic variables $\mathcal{K}$ and $\mathcal{E}$ present smoother variations than those of k and ε because the logarithm varies more slowly than its arguments. Hence, more accurate solutions can be expected when logarithmic variables are used. Examples shown latter in the paper confirm this.

The equation for $\mathcal{K}$ is obtained by first dividing the k-equation by k, and by noting that the gradient of k divided by k is equal to the gradient of $\mathcal{K}$, $[\nabla k/k = \nabla \mathcal{K}]$. The $\mathcal{E}$ and Ω equations are obtained by a similar transformation. The turbulence model equations for logarithmic variables are then as follows:

– the k–ε model of turbulence

$$\rho\, \mathbf{u}\cdot\nabla\mathcal{K} = \nabla\cdot\left[\left(\mu + \frac{\mu_T}{\sigma_k}\right)\nabla\mathcal{K}\right] + \left(\mu + \frac{\mu_T}{\sigma_k}\right)(\nabla\mathcal{K})^2 + \mu_T\, e^{-\mathcal{K}} P(\mathbf{u}) - \rho^2\, C_\mu\, \frac{e^{\mathcal{K}}}{\mu_T}$$

$$\rho\, \mathbf{u}\cdot\nabla\mathcal{E} = \nabla\cdot\left[\left(\mu + \frac{\mu_T}{\sigma_\varepsilon}\right)\nabla\mathcal{E}\right] + \left(\mu + \frac{\mu_T}{\sigma_\varepsilon}\right)(\nabla\mathcal{E})^2 + \rho\, C_{\varepsilon 1}\, C_\mu\, e^{\mathcal{K}-\mathcal{E}}\, P(\mathbf{u}) - C_{\varepsilon 2}\, \rho\, e^{\mathcal{E}-\mathcal{K}}$$

with the following definition for the eddy viscosity

$$\mu_T = \rho C_\mu e^{2\mathcal{K}-\varepsilon}$$

– the k–ω model of turbulence:

$$\rho\,\mathbf{u}\cdot\nabla\mathcal{K} = \nabla\cdot[(\mu+\sigma^*\mu_T)\nabla\mathcal{K}] + (\mu+\sigma^*\mu_T)(\nabla\mathcal{K})^2 + \mu_T e^{-\mathcal{K}} P(\mathbf{u}) - \beta^*\rho^2\frac{e^{\mathcal{K}}}{\mu_T}$$

$$\rho\,\mathbf{u}\cdot\nabla\Omega = \nabla\cdot[(\mu+\sigma\mu_T)\nabla\Omega] + (\mu+\sigma\mu_T)(\nabla\Omega)^2 + \alpha\rho e^{-\Omega}P(\mathbf{u}) - \beta\rho e^{\Omega}$$

with the following definition for the eddy viscosity:

$$\mu_T = \rho e^{\mathcal{K}-\Omega}$$

Note that the use of logarithmic variables has removed the troublesome division by ε or Ω in the eddy viscosity and replaced it by a subtraction of argument to the exponential function. Also, a number of other worrisome divisions have been removed from the differential equations for the turbulence variables. The price to pay for this advantage is the appearance of exponentials in the right hand side of the turbulence equations. However, since k and ε take on small values, the exponential is very flat so that the nonlinearities are usually very mild. In fact, our experience indicates that the use of logarithmic variables significantly enhances convergence of the solver.

4. FINITE ELEMENT FORMULATION

The finite element equations are obtained by multiplying the differential equations by suitable test functions and applying the divergence theorem to diffusion terms. This leads to the following Galerkin variational equations:

– momentum and continuity

$$(\rho\,\mathbf{u}\cdot\nabla\mathbf{u},\mathbf{v}) + a(\mathbf{u},\mathbf{v}) - (p,\nabla\cdot\mathbf{v}) = (\rho\mathbf{f},\mathbf{v}) + <t^*,\mathbf{v}>$$
$$(q,\nabla\cdot\mathbf{u}) = 0$$

with

$$(h,g) = \int_V h\,g\,\mathrm{d}V$$

$$a(\mathbf{u},\mathbf{v}) = \int_V (\mu+\mu_T)\,[\nabla\mathbf{u}+\nabla\mathbf{u}^T]:\nabla\mathbf{v}\,\mathrm{d}V$$

$$<t^*,\mathbf{v}> = \int_{\partial K\setminus\Gamma_t} [(\mu+\mu_T)(\nabla\mathbf{u}+\nabla\mathbf{u}^T)\cdot\mathbf{n} - p\,\mathbf{n}]\cdot\mathbf{v}\,\mathrm{d}s + \int_{\partial K\cap\Gamma_t} \tau_w\cdot\mathbf{v}\,\mathrm{d}s$$

where $\partial K\setminus\Gamma_t$ denotes either a freestream or outflow boundary and $\partial K\cap\Gamma_t$ represents the portion of the boundary where the law of the wall will be applied. The imposed wall shear stress boundary condition is treated implicitly and linearized with Newton's method.

The finite element formulation for turbulence models equations in logarithmic variables are as follows:

– the k–ε model

$$\int_V \Big[\rho\,\mathbf{u}\cdot\nabla\mathcal{K}\,w + \Big(\mu+\frac{\mu_T}{\sigma_k}\Big)\nabla\mathcal{K}\cdot\nabla w - \Big(\mu+\frac{\mu_T}{\sigma_k}\Big)(\nabla\mathcal{K})^2 w - \mu_T e^{-\mathcal{K}}P(\mathbf{u})\,w + \rho^2 C_\mu\frac{e^{\mathcal{K}}}{\mu_T}w\Big]\mathrm{d}V = 0$$

$$\int_V \Big[\rho\,\mathbf{u}\cdot\nabla\mathcal{E}\,w + \Big(\mu+\frac{\mu_T}{\sigma_\varepsilon}\Big)\nabla\mathcal{E}\cdot\nabla w - \Big(\mu+\frac{\mu_T}{\sigma_\varepsilon}\Big)(\nabla\mathcal{E})^2 w - \rho C_{\varepsilon 1} C_\mu e^{\mathcal{K}-\mathcal{E}}P(\mathbf{u})\,w + C_{\varepsilon 2}\rho e^{\mathcal{E}-\mathcal{K}}w\Big]\mathrm{d}V = 0$$

– the k–ω model

$$\int_V \Big[\rho\,\mathbf{u}\cdot\nabla\mathcal{K}\,w + (\mu+\sigma^*\mu_T)\nabla\mathcal{K}\cdot\nabla w - (\mu+\sigma^*\mu_T)(\nabla\mathcal{K})^2 w - \mu_T e^{-\mathcal{K}}P(\mathbf{u})\,w + \rho^2\beta^*\frac{e^{\mathcal{K}}}{\mu_T}w\Big]\mathrm{d}V = 0$$

$$\int_V \Big[\rho\,\mathbf{u}\cdot\nabla\Omega\,w + (\mu+\sigma\mu_T)\nabla\Omega\cdot\nabla w - (\mu+\sigma\mu_T)(\nabla\Omega)^2 w - \alpha\rho e^{-\Omega}P(\mathbf{u})\,w + \beta\rho e^{\Omega}w\Big]\mathrm{d}V = 0$$

The momentum and continuity equations are discretized using the seven node triangle which uses enriched quadratic shape functions for velocity and a piecewise linear and discontinuous approximation for the pressure. Turbulence equations are discretized using quadratic shape functions.

The momentum and turbulence transport equations are dominated by convection and it is well known that a standard Galerkin discretization leads to oscillations in the solutions. Hence, some form of upwinding is required to suppress these non-physical oscillations. Here we use a Streamline-Upwind/Petrov-Galerkin (SUPG) method as described by Hughes et al. [19, 20]. In this approach the test functions for momentum and turbulence equations are modified as follows:

$$w_i = N_i + \tau\,\mathbf{u}\cdot\nabla N_i$$

and therefore are different from the interpolation functions N_i. Here τ is a stabilization parameter defined as [20]:

$$\tau = \frac{\delta\,h}{2\,|V|}$$

where h is the element size, $|V|$ is the norm of the velocity and δ is a parameter depending on the local Péclet number:

$$\delta = \coth(Pe) - \frac{1}{Pe}$$

$$Pe = \frac{\rho\, h\, |V|}{2\,\lambda}$$

with λ being the diffusion coefficient of the transport equation under consideration. The additional SUPG contributions are discontinuous across element faces, consequently terms containing them will be integrated only on the element interiors.

5. ADAPTIVE METHODOLOGY

5.1. Generalities

Most adaptive methods assess the quality of an initial solution obtained on a coarse mesh by using some form of error estimation and modify the structure of the numerical approximation in a systematic fashion to improve the overall quality of the solution. In this work error estimates are obtained for all dependent variables (velocity, pressure and turbulence variables) by a local least-squares projection method as proposed by Zienkiewicz et al. [21–23]. Mesh adaptation is performed by global remeshing because it provides great control over the mesh grading to accurately resolve the flow features. In this approach the problem is first solved on a coarse mesh capable of roughly resolving the physics of the flow. The solution is analyzed to determine where more grid points are required and an improved mesh is generated. The problem is solved again on the new mesh using the previous solution as an initial guess. This process is repeated until a sufficiently accurate solution is obtained.

5.2. Error Estimation and Adaptive Remeshing

The adaptive remeshing procedure described by Ilinca et al. [16, 24] is used to cluster grid points in regions of rapid variations of all dependent variables: velocity, pressure, logarithmic turbulence variables and the eddy viscosity. Error estimates are obtained by a local least squares reconstruction of the solution derivatives [21, 22]. In the case of the velocity field the strain rate tensor is used for error estimation. An error estimate of the pressure solution is obtained by local projection of the pressure field itself. Error estimates are obtained for turbulence variables by projecting the finite element derivatives of $\mathcal{K}$, $\mathcal{E}$ and/or Ω into a continuous field. Finally, an error estimate for the eddy viscosity is also constructed since slowly varying fields of $\mathcal{K}$ and $\mathcal{E}$ can result in rapid variation of the eddy viscosity. This is very important to the success of adaptation in turbulent flows since the eddy viscosity is the sole mechanism for transfer of momentum and turbulence kinetic energy by turbulent fluctuations. See references [1, 2, 12] for examples and some discussion of these issues. This approach was successfully applied by the authors to the k–ε model [12], the k–ω model of turbulence [24, 25], to turbulent heat transfer [26] and to a pressure based finite element solution algorithm for compressible subsonic viscous flows [27].

Once the error estimates are obtained for all variables, there remains to design a better mesh. The adaptive remeshing strategy is modeled after that proposed by Peraire et al. [28]. In our approach all variables are analyzed and contribute to the mesh adaptation process. The mesh characteristics (element size) are derived for each variable on a given element. The minimum element size predicted by each of the dependent variable is selected on each element. Details of the steps of this algorithm are presented in reference [16].

5.3. Logarithmic variables and solution errors

The effect of the change of dependent variables on the solution accuracy can be best appreciated by looking at the relationship between the error in a given turbulence variable and the error in its natural logarithm. Let e_k and $e_\mathcal{K}$ denote the error in k and in its natural logarithm, $\mathcal{K}$, respectively. We have the following relationships between the exact solution and its logarithm:

$$k_{\mathrm{ex}} = e^{\mathcal{K}_{\mathrm{ex}}}$$

We also have the following relationship between the exact values and their finite element approximation:

$$k_{\mathrm{ex}} = k_{\mathrm{h}} + e_k\,, \qquad \mathcal{K}_{\mathrm{ex}} = \mathcal{K}_{\mathrm{h}} + e_\mathcal{K}$$

We can then write

$$k_{\mathrm{h}} + e_k = e^{\mathcal{K}_{\mathrm{h}} + e_\mathcal{K}} = e^{\mathcal{K}_{\mathrm{h}}}\, e^{e_\mathcal{K}} = e^{\mathcal{K}_{\mathrm{h}}}\,(1 + e_\mathcal{K} + \mathcal{O}(e_\mathcal{K}^2))$$

Which, upon neglecting higher order terms, leads to

$$k_{\mathrm{h}} + e_k \approx k_{\mathrm{h}} + k_{\mathrm{h}}\, e_\mathcal{K}$$

That is

$$e_k \approx k_{\mathrm{h}}\, e_\mathcal{K}$$

In other words, the error in the logarithm of k is proportional to the relative error in k. This observation plays a significant role for turbulent flows. Recall that the mesh adaptation strategy uses the principle of equi-distribution of the error. Recall also that k is often very small in the free stream. With the use of logarithmic variables the solver and the error estimation process

will easily see the significance of an error estimate of 10^{-6} in a region where k is of order 10^{-6}, and the mesh will be refined in that region. In other words, logarithmic variables will detect regions where the error is sizable when compared to the norm of the solution. This is not the case when using k as a dependent variable. This reasoning also holds for ε and for ω, and is also applicable to the non-linear finite element equation solver. In the last case this results in more accurate solution of the discrete nonlinear equations.

When using k and ε as dependent variables, small errors in regions of low turbulence variables can have disastrous effects on the accuracy of the eddy viscosity. Indeed, since the eddy viscosity is given by

$$\mu_T = \rho C_\mu \frac{k^2}{\varepsilon}$$

the error in the eddy viscosity can be written as

$$\frac{e_{\mu_T}}{\mu_T} = 2\frac{e_k}{k} - \frac{e_\varepsilon}{\varepsilon}$$

which shows that the relative errors in k and ε accumulate in that of the eddy viscosity. This means that a 5 percent uncertainty in k and ε results in a 15 percent error in eddy viscosity. Furthermore, the error in eddy viscosity can be amplified by the division if k and/or ε are small. This amplification can have disastrous effects especially in the free stream of flows over airfoils or in free shear layers. It is straightforward to show that when logarithmic variables are used the relationship between the eddy viscosity error and the error in the logarithmic variables is given by

$$e_{\mu_T} = \mu_T (2\, e_K + e_\mathcal{E})$$

This shows that the error estimation in the eddy viscosity will no longer be affected by the local level of the turbulence variables and is no longer subject to the numerical difficulties associated with division by small numbers. This explain in part the ability of the proposed method on coarse meshes.

6. APPLICATIONS

6.1. A shear layer with a closed form solution

This problem served as a validation case in reference [1] to test the accuracy of the error estimation technique. In this flow the eddy viscosity is a linear function of x and is independent of y.

$$u = \frac{u_1 + u_2}{2} - \frac{u_1 - u_2}{2}\,\mathrm{erf}(\frac{\sigma y}{x})$$

$$v = \frac{u_1 - u_2}{2}\,\frac{1}{\sigma\sqrt{\pi}}\,\exp\left[-\left(\frac{\sigma y}{x}\right)^2\right]$$

$$p = 0$$

$$k = k_0\left\{c_k + \exp\left[-\left(\frac{\sigma\, y}{x}\right)^2\right]\right\}$$

$$\varepsilon = \frac{\varepsilon_0}{x}\left\{c_k + \exp\left[-\left(\frac{\sigma y}{x}\right)^2\right]\right\}^2$$

$$\mu_T = \mu_{T_0}\, x$$

The constants are taken to be

$$u_1 = 1.0\,, \qquad u_2 = 0.0\,, \qquad \sigma = 13.5$$

$$k_0 = \frac{343}{75\,000}\,u_1\,(u_1 - u_2)\,\frac{\sigma}{\sqrt{\pi}}\,, \qquad c_k = \frac{2{\cdot}10^{-3}}{k_0}\,,$$

$$\varepsilon_0 = \frac{343}{22\,500} C_\mu\, u_1\,(u_1 - u_2)^2\,\frac{\sigma^2}{\pi}$$

$$\mu_{T_0} = \frac{343}{250\,000}\,\rho\, u_1\,, \qquad Re_l = \frac{\rho\, u_1\, L}{\mu_l} = 10^4$$

The computational domain is the rectangle [100, 300] × [−75, 75]. The problem was solved first in logarithmic variables and then with the standard form of the k–ε model. All equations are solved using the SUPG formulation.

The meshes generated by the adaptive procedure are shown in *figure 1*. On the last mesh several diagonal bands of refinement can be clearly seen. They correspond to regions of rapid variation in velocity, $\mathcal{K}$, $\mathcal{E}$, and μ_T. The same meshes have been used to compute the solution using (k, ε) and ($\mathcal{K}$, $\mathcal{E}$) as dependent variables. In this way, we can compare the accuracy of the eddy viscosity obtained using both approaches. *Figure 2* presents the trajectory of the true error for the eddy viscosity. As can be seen, the use of logarithmic variables leads to a far more accurate prediction of the eddy viscosity than the classical solution approach. This fact is illustrated on *figure 3* which shows the eddy viscosity field obtained on first mesh. The plot on the top illustrates results from the (k, ε) solution, while the second one presents the solution obtained using logarithmic variables. The exact solution is presented on the bottom. All plots contain 20 contour lines from 0.1372 to 0.4116. As can be seen, logarithmic variables lead to significant improvements in the quality of the eddy viscosity distribution. This is mainly due to the fact that a quadratic interpolation of the logarithm of turbulence quantities is more accurate than a quadratic interpolation of the turbulence quantities themselves in regions of rapid variations. While improvements in the accuracy of the solution are more pronounced on

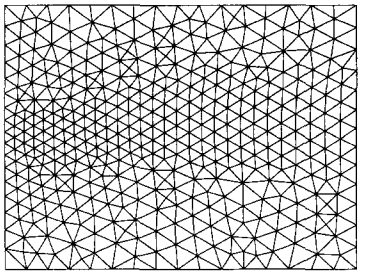

Mesh-0

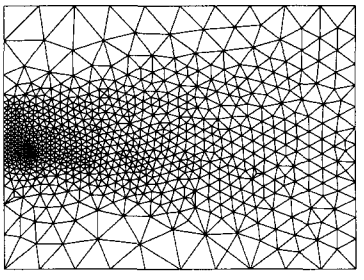

Mesh-1

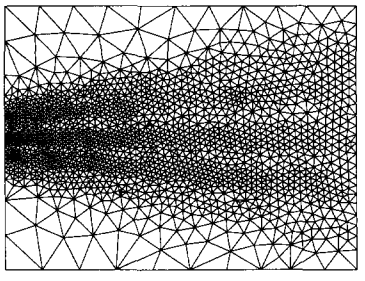

Mesh-2

Figure 1. Meshes for the analytical shear layer.

coarser meshes, *figure 2* shows that the solutions using logarithmic variables are always more accurate on any mesh than those obtained from the (k, ε) calculation.

6.2. Flow over a backward facing step

This problem was studied experimentally by Westphal et al. [29]. The geometry and boundary conditions are shown in *figure 4*. All geometrical values are dimensionless with the reference length being the step height H. The Reynolds number based on the inlet mean velocity and the step height is $Re = (U \cdot H)/\nu = 42\,000$. The inlet turbulence intensity is set to 2 % $(k/U^2 = 0.02)$. The distance to the wall is 0.02 resulting in a y^+ value between 30 and 100 on all solid boundaries. The initial mesh, shown in *figure 5*, is very coarse having only two elements along the step height and four in the upstream channel. This is an indication of the robustness of the

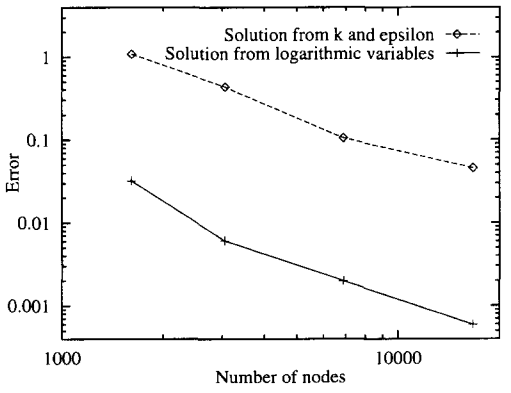

Figure 2. Trajectory of the eddy viscosity error for the analytical shear layer.

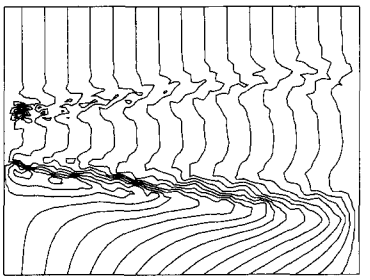

Solution from k and ϵ

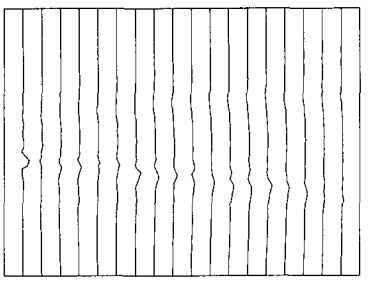

Solution from logarithms ($\mathcal{K}$ and $\mathcal{E}$)

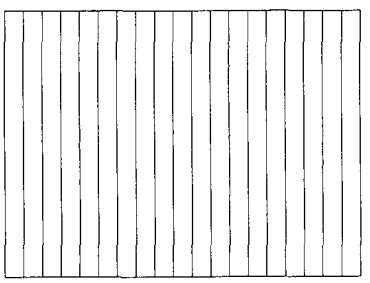

Exact solution

Figure 3. Analytical shear layer: contour lines of the turbulent viscosity on the first mesh.

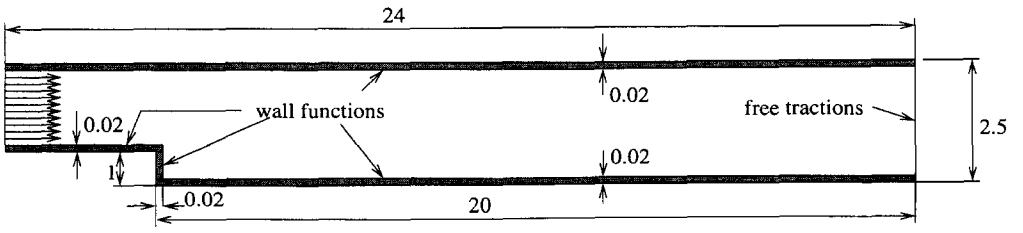

Figure 4. Computational domain for the backward facing step.

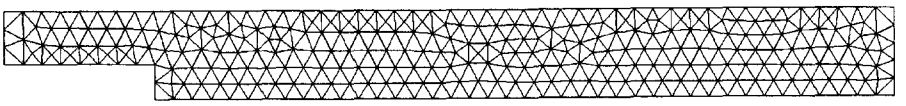

Figure 5. Initial mesh for the backward facing step.

flow solver arising from the use of logarithmic variables. The solution obtained on this mesh is not very accurate but is sufficiently smooth to properly drive adaptivity so that grid points are automatically concentrated on regions of rapid changes of the solution. There is no need for grid clustering on the initial mesh using a priori knowledge of the solution behavior. Moreover, because the solution is interpolated between two subsequent meshes, the procedure is also cost effective.

The adaptive procedure was completed for the two turbulence models separately. *Figures 6* and *7* show the final meshes and contours of the turbulent kinetic energy logarithm and of the eddy viscosity for the k–ε and k–ω models. As can be seen the final meshes are comparable. The final meshes contain 25 337 nodes and 12 290 elements for the k–ε model, and 26 382 nodes and 12 803 elements for the k–ω model. Grid points are clustered in the shear layer emanating from the corner of the step where all variables exhibit strong variations. Elements are also clustered in the boundary layers along solid walls because of the rapid changes in the turbulent viscosity. The final solution is very smooth in both cases.

The length of the recirculation zone is compared with experimental data in the *table*. The predictions using the k–ε model are closer to experimental data on adapted meshes. The k–ω model prediction is farther from the data. The cause for this behavior may be the absence of a cross derivative term in the ω-equation. For both models the difference between the values obtained on the last two adapted meshes, (mesh 2 and 3), is very small indicating that the solutions are grid independent.

Figure 8 compares numerical predictions and experimental data for the x-component of velocity at four control stations. Following Westphal et al. [29] on the x-axis we plot the u velocity normalized by its maximum value at that section, while on the y-axis we have the dimensionless y coordinate. Results from the last two adapted meshes are plotted. As can be seen there are practically no differences between the solutions on those two meshes. This indicates that the adaptive process has resulted in grid independent solutions. In the recirculation zone, the k–ε model provide a better velocity prediction than the k–ω model. This is in agreement with the previous observation concerning the underestimation of the recirculation length of the k–ω model.

TABLE
Length of the recirculation zone.

Model/experiment	Length	error (%)
Experiment[29]	7.33 ± 1.0	13.6
k–ε, mesh – 0	3.90	46.8
k–ε, mesh – 1	6.07	17.2
k–ε, mesh – 2	6.43	12.3
k–ε, mesh – 3	6.47	11.7
k–ω, mesh – 0	5.97	18.5
k–ω, mesh – 1	6.51	11.2
k–ω, mesh – 2	5.81	20.7
k–ω, mesh – 3	5.88	19.8

Figure 9 presents profiles of the TKE. The values are normalized by the maximum value of the TKE in each section as provided in the experimental data. The station located at $x/H = 4$ is in the recirculation zone while the other three are positioned downstream of the reattachment point. Both models behave in the same way and result in predictions close to experiment.

7. CONCLUSION

This paper has presented a change of dependent variables which guarantees positivity of turbulence variables in two-equation models of turbulence.

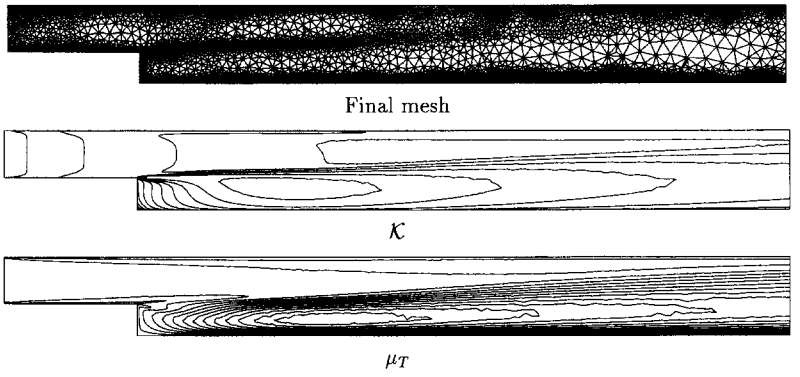

Figure 6. Backward facing step: final mesh and solution for the k–ε model.

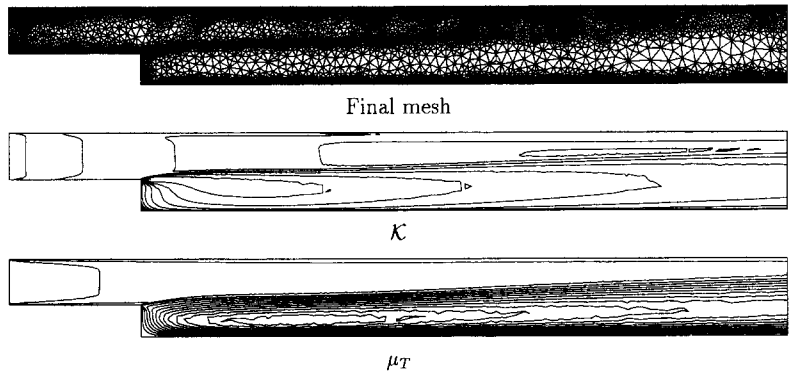

Figure 7. Backward facing step: final mesh and solution for the k–ω model.

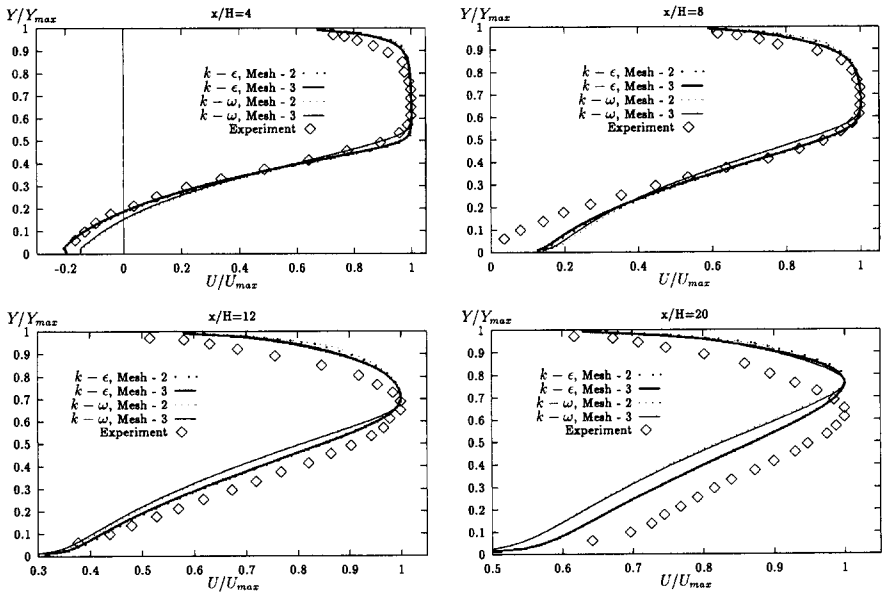

Figure 8. Velocity profiles for the backward facing step.

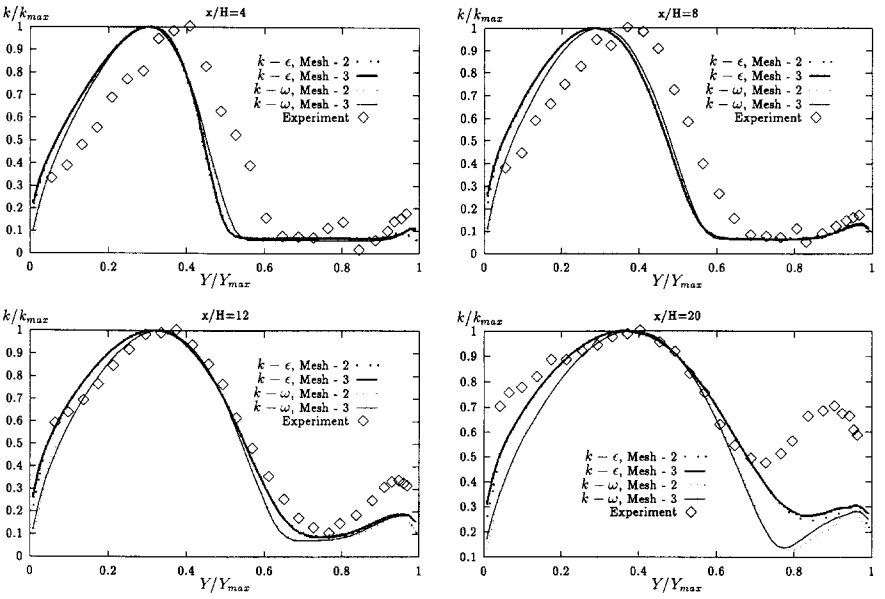

Figure 9. TKE profiles for the backward facing step.

The use of logarithmic variables for turbulence quantities eliminates the need for clipping or limiting turbulence variables from below in the course of numerical iteration. The use of logarithmic variables presents the following advantages over standard variables:

- turbulence quantities are always positive;
- the eddy viscosity never becomes negative;
- solutions can be obtained on coarser initial meshes;
- logarithmic variables vary more slowly than k, and ε; hence, resolution of fronts in turbulence variables and eddy viscosity is improved;
- adaptation using error estimates in logarithmic variables lead to significant improvement in accuracy of the solution in regions where turbulence quantities are extremely small.

Numerical experiments have shown that the use of logarithmic variables leads to improved prediction of the eddy viscosity field on problems having an analytical solution, and for practical turbulent flows. This is due to the combined effect of improved resolution resulting from the use of logarithmic variables and to the elimination of clipping in the solution algorithm.

Acknowledgment

This work was supported in part by the Natural Sciences and Engineering Research Council, Canada (NSERC), Fonds de formation des chercheurs et d'aide à la recherche (FCAR), and the US Air Force Office of Scientific Research (AFOSR) Grant F49620-96-1-0329.

REFERENCES

[1] Illinca F., Pelletier D., Garon A., An adaptive finite element method for a two-equation turbulence model in wall bounded flows, Int. J. Num. Meth. Fluids 24 (1) (1997) 101–120.

[2] Ilinca F., Pelletier D., Arnoux-Guisse F., An adaptive finite element scheme for turbulent free shear flows, Int. J. CFD 8 (3) (1997) 171–188.

[3] Menter F.R., Zonal two-equation k–ω turbulence models for aerodynamic flows, in: 24th AIAA Fluid Dynamics Conference, 1993, AIAA Paper 93-2906.

[4] Yang Z., Shih T.H., A Gallilean and tensorial invariant k–ε model for near-wall turbulence, in: 94th AIAA Fluid Dynamics Conférence, 1993, AIAA Paper 93-3105.

[5] Shur M., Strelets M., Zaikov L., Gulyaev A., Kozlov V., Secundov A., Comparative testing of one- and two-equation turbulence models for flows with separation and reattachment, in: 33rd AIAA Acrospace Sciences Meeting and Exhibit, Jan. 1995, AIAA Paper 95-0863.

[6] Jacon F., Knight D., A Navier-Stokes algorithm for turbulent flows using an unstructured grid and flux difference splitting, in: 25th AIAA Fluid Dynamics Conference, 1994, AIAA Paper 94-2293.

[7] Mohammadi B., Pironneau O., Analysis of the k-epsilon turbulence model, John Wiley & Sons, 1994.

[8] Spalart P., Allmaras S.R., A one-equation turbulence model for aerodynamic flows, Jan. 1992, AIAA Paper 92-0439.

[9] Baldwin B.S., Barth T.J., A one-equation turbulence transport model for high Reynolds number wall-bounded flows, Report NASA TM-102847, 1990.

[10] Launder B.E., Spalding D.B., Mathematical Models of Turbulence, Academic Press, London, 6th ed., 1972.

[11] Wilcox D.C., Turbulence Modeling for CFD, La Canada, California, DCW Industries, 1993.

[12] Pelletier D., Ilinca F., Adaptive remeshing for the k–ε model of turbulence, AIAA J. 35 (4) (1997) 640–646.

[13] Pelletier D., Ilinca F., Hétu J.-F., Adaptive remeshing for convective heat transfer with variable fluid properties, J. Thermophys. Heat Tr. 8 (4) (1994) 687–694.

[14] Pelletier D., Ilinca F., Hétu J.-F., Adaptive finite element method for turbulent flow near a propeller, AIAA J. 32 (11) (1994) 2186–2193.

[15] Kim S.E., Choudhury D., Computations of complex turbulent flows and heat transfer using two-layer based wall functions, in: Proceedings of the 30th National Heat Transfer Conference, 1995.

[16] Ilinca F., Méthodes d'éléments finis adaptatives pour les écoulements turbulents, Thesis, École polytechnique de Montréal, March 1996.

[17] Bristeau M.O., Glowinski R., Dimoyat B., Periaux J., Perrier P., Pironneau O., Finite element methods for the compressible Navier–Stokes equations, in: AIAA Computational Fluid Dynamics Conference, 1983, AIAA-83-1890.

[18] Fortin M., Manouzi H., Soulaimani A., On finite element approximation and stabilization methods for compressible viscous flows, Int. J. Numer. Meth. Fluids 17 (1993) 477–499.

[19] Brooks A.N., Hughes T.J.R., Streamline upwind/ Petrov–Galerkin formulations for convective dominated flows with particular emphasis on the incompressible Navier–Stokes equations, Comput. Meth. Appl. M. 32 (1982) 199-259.

[20] Hughes T.J.R., Franca L.P., Balestra M., A new finite element formulation for computational fluid dynamics. V. Circumventing the Babuška-Brezzi condition: a stable Petrov–Galerkin formulation of the Stokes problem accommodating equal-order interpolations, Comput. Meth. Appl. M. 591 (1986) 85—99.

[21] Zienkiewicz O.C., Zhu J.Z., The superconvergent patch recovery and a posteriori error estimators. Part 1: The recovery technique, Int. J. Numer. Meth. Eng. 33 (7) (1992) 1331–1364.

[22] Zienkiewicz O.C., Zhu J.Z., The superconvergent patch recovery and a posteriori error estimators. Part 2. Error estimates and adaptivity, Int. J. Numer. Meth. Eng. 33 (7) (1992) 1365–1382.

[23] Zienkiewicz O.C., Zhu J.Z., The superconvergent patch recovery (SPR) and adaptive finite element refinement, Comput. Meth. Appl. Mech. Eng. 101 (1-3) (1992) 207–224.

[24] Ilinca F., Pelletier D., Garon A., Positivity preserving formulations for adaptive solution of two-equation models of turbulence, in: 27th AIAA Fluid Dynamics Conference, (New Orleans, LA), June 1996, AIAA Paper 96-2056.

[25] Pelletier D., Garon A., Ilinca F., Adaptive finite element algorithms for the k–ε and k–ω models of turbulence, in: Advances in Finite Element Analysis in Fluid Dynamics, Proceedings of the ASME Winter Annual Meeting, 1994.

[26] Ignat L., Pelletier D., Ilinca F., An adaptive finite element method for turbulent heat transfer, in: 34th AIAA Aerospace Sciences Meeting and Exhibit, (Reno, NV), January 1996, AIAA Paper 96-0607.

[27] Ilinca F., Pelletier D., A pressure based adaptive finite element algorithm for compressible viscous flows, in: 34th AIAA Aerospace Sciences Meeting and Exhibit (Reno, NV), January 1996, AIAA Paper 96-0679.

[28] Peraire J., Vahdati M., Morgan K., Zienkiewicz O.C., Adaptive remeshing for compressible flow computations, J. Comput. Phys. 72 (2) (1987) 26–37.

[29] Westphal R.V., Johnston J.P., Eaton J.K., Experimental study of flow reattachement in a single-sided sudden expansion, Tech. Rep. NASA 3765, Report MD-41, Stanford University, 1984.